Quantifying photosynthetic restrictions

Chandra Bellasio

Laboratory of Theoretical and Applied Crop Ecophysiology, School of Biology & Environmental Science, University College Dublin, Belfield, Dublin 4, Dublin; Biology of plants under Mediterranean conditions; Department of Chemistry, Biology and Biotechnology, Università Degli Studi di Perugia, Perugia, 06123, Italy; Department of Biology, University of the Balearic Islands 07122 Palma, Illes Balears, Spain; Research School of Biology, The Australian National University, Acton, ACT, 2601 Australia. ORCID: 0000-0002-3865-7521. chandra.bellasio@ucd.ie

Keywords

Modelling; partitioning; contribution; limitation; control, sensitivity; stomatal; non-stomatal; mesophyll; biochemical, non-diffusional

Abstract

Quantifying the effect of factors controlling CO_2 assimilation is crucial for understanding plant functions and developing strategies to improve productivity. Methods exist in numerous variants and produce various indicators, such as limitations, contributions, and sensitivity, often causing confusion. Simplifications and common mistakes lead to overrating the importance of diffusion – whether across stomata or the mesophyll. This work develops a consistent set of definitions that integrates all previous methods, offering a generalised framework for quantifying restrictions. Twelve worked examples are provided in a free downloadable spreadsheet, demonstrating the simplicity and applicability to a wide range of questions.

Introduction

Photosynthetic gas exchange routines measure CO_2 uptake (assimilation, A) and water vapour release (transpiration, E), under a range of external CO_2 concentration and light intensities (Busch 2018). Raw data is first processed using classical calculations embedded in the gas analyser software (von Caemmerer and Farquhar 1981), or their recent upgrade (Márquez et al. 2021), to derive stomatal conductance to CO_2 (g_S), together with the CO_2 concentration in the substomatal cavity (C_i). Further analysis uses mathematical models, validated by associating macroscopic data patterns with leaf properties, then adjusted to match data through curve fitting procedures (Bellasio et al. 2016b; Bellasio et al. 2016a). Since these approaches estimate physical or biochemical quantities representing actual characteristics of leaves, their performance can be quantitatively evaluated. (For instance, by direct experimental comparison with more accurate procedures or through *in silico* experiments that measure the capacity of the method to reproduce the known starting parameterization from a synthetic dataset (Gu and Sun 2014).) Alternative approaches

involve identifying and quantifying those factors that restrict assimilation. These seek to gain insights into the state of the process rather than estimating the quantities defining it. Various methods based on different assumptions and conventions abound in the literature, and the lack of an objective criterion for their selection often renders the choice of methods "*to some extent arbitrary*" (Jones 1985). My aim is to establish a framework with general validity that is straightforward to implement and unambiguous.

The theoretical basis of restriction analysis were laid by Gaastra (1959) and were developed in the 1970s (Jarvis 1971; Jones 1973; Jones and Slatyer 1972; Prioul and Chartier 1977). Early studies made the erroneous assumption that CO_2 concentration at the mesophyll carboxylating sites (C_M) is zero. Biochemical CO_2 uptake was treated as a linear function akin to electrical resistance (Ohm's Law). However, it typically responds non-linearly with a saturating response to CO_2, therefore as Farquhar and Sharkey (1982) noted, this "*linear resistance analysis is in most cases invalid*". In addition, rather than conveying information about the process, resistance confounds with a physical characteristic, making it difficult to relate to the sought process information. Consequently, I deem these methods undesirable and I will not address them further.

The concept of restriction was also related to that of mathematical sensitivity, for review Jones (1985). Both the analysis of absolute and relative sensitivity (elasticity) quantify the extent to which various input variables (such as C_i) exert control over the process of assimilation. Control analyses are applicable only to infinitesimal change. This has the benefit that, if model parameterization is defined, outputs are unequivocal (Jones 1973). The drawback is that control coefficients are relatively difficult to derive and relate to actual physiological phenomena. Often, the information sought pertains to finite changes between two well-identifiable conditions of interest. For instance, a first common approach called limitation analysis involves comparing a healthy plant with its potential attainable under idealized conditions. The analysis quantifies the gain in assimilation achieved by sequentially 'lifting' limitations until photosynthesis reaches its maximum. Alternatively, contribution analysis compares a healthy plant with the same or a similar plant after the imposition of a treatment. The analysis attributes the changes in assimilation to the various variables responsible for causing the change.

Extending sensitivity analysis to those finite changes introduces error (Deans et al. 2019), but it is a practice that has been widely used both for C_3 plants (Grassi and Magnani 2005) and in the C_4 variant (Cano et al. 2019). Error is amplified when the required slopes of the A/C_i response are misestimated as in Tomás et al. (2013). Despite the foresight of Prioul et al. (1984) who proposed to evaluate many small steps, the need to derive assimilation graphically and simplify manual data processing meant that most studies calculated assimilation in only three points. This raised the issue that the order in which these points are evaluated influences the result of the analysis (path dependency). Key advancements have been replacing drawn curves with a computerised routine that fitted empirical models (Bellasio et al. 2016b). This approach was later extended to compare C_4

and C_3 plants but remained limited, as it used the classical three-point calculation, and was only applied to stomatal and non-stomatal limitations (Bellasio et al. 2018). Buckley and Diaz-Espejo (2015) increased the number of points to any large number presenting an infinitesimal numerical computerised method. It had the main benefits of being unambiguous, avoiding linearization of assimilatory responses over finite intervals, and implicitly containing sensitivity, thereby reconciling contribution with control analysis. However, it only applied to contribution analysis in C_3 plants, leaving the need for a method that is universally applicable.

I will develop a unified theory and terminology that can be used to analyse controls, limitations and contributions in all plants, and show the implementation of common procedures in spreadsheets freely available for download, demonstrating the framework's simplicity and applicability to a wide range of questions..

Theory: constructing a general framework

First, hypothesize a healthy plant photosynthesizing under ordinary operational conditions (Figure 1a). To assess the extent to which ordinary restrictions limit the plant relative to its potential, a limitation analysis (number 1 in Figure 1a) can be conducted. This analysis simulates a transition along a hypothetical dimension that lifts all restrictions. At any given intermediate point along this transition, a control analysis (a 'C' in Figure 1a) can be performed to determine the extent to which an infinitesimal change in the transition is controlled by environmental drivers and the underpinning photosynthetic characteristics.

Second, consider a set of plants subjected to a generic treatment and left to photosynthesize under the same ordinary operational conditions as the healthy plants. To quantify the influence of the physiological characteristics affected by the treatment on assimilation under operational conditions, a contribution analysis (number 2 in Figure 1a) is conducted. This analysis simulates a transition that reverts the treatment, breaking the change in assimilation into contributions assigned to the drivers causing it.

Alternatively, to assess the extent to which treated plants are limited under ordinary conditions relative to their potential, a limitation analysis on treated plants (number 3 in Figure 1a) can be conducted. Any residual difference between the potential of the treated plant and that of the healthy plant can be evaluated through a transition that reverts the treatment, but this time in idealized conditions (number 4 in Figure 1a).

The strength of this new generalized framework lies in its ability to combine restriction analyses. For instance, in a time-course experiment where a plant undergoes progressive treatment and is sampled at subsequent time points, limitation analysis can be performed at each time point, while contribution analysis can be used to compare these subsequent time points. Control analysis can be overlaid for each infinitesimal step along both the real and hypothetical trajectories.

To formalize this framework, it is necessary to assume that photosynthesis can be described mathematically. Let the function *f* be a set of expressions describing the dependence of any generic output variable Ω on a set of inputs, which are termed *a* (a generic input variable) and $\boldsymbol{b}$ (the set of all other inputs):

$$\Omega = f(a, \boldsymbol{b}) \qquad 1$$

This is exemplified by the red line in Figure 2, which plots the values of Ω on the ordinate as a function of *a* on the abscissa, obtained for the specific parameterization set $\boldsymbol{b}_{\mathrm{I}}$. Any situation with well-defined conditions, where *a* and $\boldsymbol{b}$ are known, will be referred to as a 'state'. These may be the healthy and treatment operational conditions, or the hypothetical scenarios in which limitations are progressively lifted. Only a few states are typically of interest, but, let the number of states be any integer *M*, with *m* being any generic state counted in Roman numbers ($m = I, II, III \ldots . M$).

Any transition between two states is divided in a number of intervals *K*, being the total number of intervals, with *k* being any generic intermediate interval counted in integers ($k = 0, 1, 2, 3 \ldots . K$). In Figure 2, the transition between state I and state II is divided in *K* = 4 intervals.

Following Buckley and Diaz-Espejo (2015) the value of a generic input in the interval *k* scales linearly between the values in the two adjacent known states *m* and *m*+I as:

$$a_{\mathrm{m,k}} = a_{\mathrm{m}} + \frac{k}{K}(a_{\mathrm{m+I}} - a_{\mathrm{m}}), \qquad 2$$

and the calculation is analogous for all other inputs in the set $\boldsymbol{b}$.

Within the interval *k* to *k*+1 the 'Marginal Contribution of *a* to the change in Ω' is defined as:

$$\xi(a)_{\Omega} = f\left(a_{\mathrm{m,k+1}}, \boldsymbol{b}_{\mathrm{m,k}}\right) - f\left(a_{\mathrm{m,k}}, \boldsymbol{b}_{\mathrm{m,k}}\right), \qquad 3$$

and is visualised in Figure 2 for the transition from $a_{\mathrm{I},2}$ to $a_{\mathrm{I},3}$. This definition of marginal contribution corresponds to that of Eqn 5b in Buckley and Diaz-Espejo (2015). Eqn 3 can be formulated in the analogous form $\xi'(a)_{\Omega} = f\left(a_{\mathrm{m,k+1}}, \boldsymbol{b}_{\mathrm{m,k+1}}\right) - f\left(a_{\mathrm{m,k}}, \boldsymbol{b}_{\mathrm{m,k+1}}\right)$ (shown in purple in Figure 2). Because $f(a, \boldsymbol{b})$ is typically non-linear, $\xi'(\Omega)_a$ differs from $\xi(\Omega)_a$ by an error ε, see Deans et al. (2019). For instance, in Figure 2 $\xi'(a)_{\Omega}$ is 30% higher than $\xi(a)_{\Omega}$. ε decreases monotonically with *K*, therefore this issue vanishes when a suitably large value of *K* is chosen; hereafter *K*=1000 following Buckley and Diaz-Espejo (2015).

The key metric of contribution analysis is the 'Total Contribution of *a* to the change in Ω', which, in the transition from state I to state *M*, is the sum of the marginal contributions over all intermediate intervals and states:

$$\Xi(a)_{\Omega} = \sum_{m=\mathrm{I}}^{M} \sum_{k=0}^{K} \xi(a)_{\Omega} . \qquad 4$$

This definition of total contribution corresponds to that of Eqn 5c in Buckley and Diaz-Espejo (2015).

The 'Relative Contribution of a to the change in Ω' between the state I and the state M is:

$$\rho(a)_{\Omega} = \frac{\Xi(a)_{\Omega}}{\Omega_{\mathrm{M,K}} - \Omega_{\mathrm{I,0}}}. \qquad 5$$

The definition of relative contribution corresponds to Eqn 25 in Jones (1985).

The key metric in limitation analysis is the 'Limitation by a to the change in Ω', which, between the state I and the state M is:

$$L(a)_{\Omega} = \frac{\Xi(a)_{\Omega}}{\Omega_{\mathrm{M,K}}}. \qquad 6$$

This definition of limitation corresponds to Eqn 13 in Jones (1985), and Eqn 13 in Farquhar and Sharkey (1982), and to Eqn 7 in Buckley and Diaz-Espejo (2015) but expressed as percentage therein.

The key metrics in control analysis are absolute and relative sensitivity. The absolute 'Sensitivity of Ω to a', calculated in a particular state and interval (m, k), is:

$$S(\Omega)_{a} = \frac{\xi(a)_{\Omega}}{a_{\mathrm{m,k+1}} - a_{\mathrm{m,k}}}. \qquad 7$$

Sensitivity, a finite-difference estimate of $\frac{\partial f}{\partial a}$, corresponds to Eqn 1 in Jones (1985) and to the partial derivatives in Eqn 1 of Buckley and Diaz-Espejo (2015).

Finally, the relative sensitivity better referred to as 'elasticity of Ω to a', calculated in a particular state (m, k), is:

$$\eta(\Omega)_{a} = \frac{\ln f(a_{\mathrm{m,k+1}}, \boldsymbol{b}_{\mathrm{m,k}}) - \ln f(a_{\mathrm{m,k}}, \boldsymbol{b}_{\mathrm{m,k}})}{\ln a_{\mathrm{m,k+1}} - \ln a_{\mathrm{m,k}}}. \qquad 8$$

Elasticity, a finite-difference estimate of $\frac{\partial Ln(f)}{\partial Ln(a)}$ corresponds to Eqn 2 in Jones (1985), to the partial derivatives in Eqn 3 of Buckley and Diaz-Espejo (2015) and in Eqn 7 of Grassi and Magnani (2005).

There will be as many analogous formulations of Eqns 1 to 8 as there are model inputs. All definitions given above are generally valid, but below I will only explore the case in which the output Ω is net photosynthetic CO_2 uptake (A), and the function f is hence a model of photosynthesis.

Recommended applications

Diffusional and non-diffusional restrictions

The general behaviour of the ordered pairs (C_i, A) measured by gas exchange (an example is provided in Table 2), called A/C_i response curves, needs to be captured by a mathematical model of photosynthesis. Many formulations exist; these are generally grouped as mechanistic models – in which the expressions describe biochemical processes known to occur within leaves – and empirical models – in which expressions describe the fitting of data patterns. Broadly speaking, the main

difference between the two is that mechanistic models include modules describing processes. However, the distinction is not clear-cut. In mechanistic models the description of processes can be refined to virtually any desired level of detail, but ultimately will still rely on some empirical data pattern. Empirical models, on the other hand, do not explicitly formulate the underlying processes, but still describe patterns that ultimately depend on them. Empirical models may become unreliable when used in environmental conditions differing from those under which they were calibrated, and can accommodate a limited range of hypothetical scenarios. However, they are typically more accurate for describing empirical datasets and valid for all photosynthetic type. Here I will initially use the empirical model of Prioul and Chartier (1977), because it is simple, suitable for all common restriction analyses, and can be used for C_3 and C_4 photosynthesis (Bellasio et al. 2018) as well as intermediate types alike. In the modified formulation of Bellasio et al. (2016b) the dependence of assimilation upon CO_2 concentration (C) is described as:

$$A = \frac{CE\,(C - \Gamma) + A_{\mathrm{SAT}} - \sqrt{(CE[C - \Gamma] + A_{\mathrm{SAT}})^2 - (4\,\omega\,A_{\mathrm{SAT}}\,CE\,[C - \Gamma])}}{2\omega}, \qquad 9$$

where, A_{SAT} is the CO_2-saturated rate, CE is the initial slope, C may be C_{i} or C_{M} (used later), Γ is the x-intercept, ω is defining curvature. CE, Γ, and ω represent the fixed characteristics of the plant (the vector $\boldsymbol{b}$ in Eqn 1) and are found by curve fitting, that is, by inputting the measured value of C_{i} in Eqn 9 and adjusting their value until Eqn 9 outputs the output value of assimilation that is most similar to that measured. The values fitted to example data are shown in Table 2.

Stomatal limitation, the reduction of assimilation due to stomatal closure that occurs in a leaf in a real, ordinary operational conditions as compared to a hypothetical case where CO_2 would freely enter the leaf, is lifted in a single transition (number 1 in Figure 1b) between state I where C_{i} equals C_{iop}, and state II, the hypothetical scenario where C_{i} is set to the external CO_2 concentration. A numerical example is shown in Figure 3A). Calculations are shown in Sheet 1, together with control analysis, calculated for each step of the transition. The same procedure can be utilized to compare two known states resulting from any environmental perturbation (transition number 3 in Figure 1b), as long as they can be described by the same A/C_{i} response curve, simply by entering the two relevant C_{i} values in Sheet 1.

The analysis of diffusional limitation quantifies the total effect of diffusion from atmosphere to the sites of carboxylation. This includes gaseous diffusion (across stomata that through the air passages between cells), dissolution in water, and liquid diffusion (through the cell wall, plasmalemma and through the mesophyll to the sites of carboxylation, located in the chloroplasts of C_3 leaves or in the cytosol of C_4 leaves), to reach Rubisco or phosphoenolpyruvate carboxylase. The ease of this process is referred to the total conductance $g_{\mathrm{Tot}} = \frac{g_{\mathrm{S}}\,g_{\mathrm{M}}}{g_{\mathrm{S}} + g_{\mathrm{M}}}$, where mesophyll conductance (g_{M}) compunds all processes that are not stomatal. Obtaining g_{M} is not straightforward

and requires combined measurements of gas exchange and variable fluorescence in C_3 plants (Bellasio et al. 2016b), or isotopic methods in C_3 and C_4 plants (Ubierna et al. 2017; Busch et al. 2020). Diffusional limitation is evaluated in the same way as stomatal limitation, using C_M in place of C_i. Practically, for each measured value of C_i, the corresponding value of C_M is calculated as $C_M = C_i - \frac{A}{g_M}$. Eqn 9 is fitted as described above, this time to the A/C_M response curve obtaining new C_M-based CE, and ω (Table 2). Application is exemplified in Sheet 3 of the workbook.

Diffusional limitation can be further resolved in its stomatal and mesophyll components. Instead of deriving a new model, I present an addition that is generally applicable, including to the C_3 and C_4 mechanistic formulations shown below. From Eqn 3, the relative stomatal contribution to the change in C_M in any transition between two generic steps k and k+1 is:

$$\rho(g_S)_{C_M} = \frac{C_M\left(g_{S_{k+1}}, g_{M_k}\right) - C_M\left(g_{S_k}, g_{M_k}\right)}{C_M\left(g_{S_{k+1}}, g_{M_{k+1}}\right) - C_M\left(g_{S_k}, g_{M_k}\right)}. \qquad 10$$

Substituting for $C_M = C_a - \frac{A}{\frac{g_S g_M}{g_S + g_M}}$ and simplifying:

$$\rho(g_S)_{C_M} = \frac{1}{1 + \frac{\frac{1}{g_{M_{k+1}}} - \frac{1}{g_{M_k}}}{\frac{1}{g_{S_{k+1}}} - \frac{1}{g_{S_k}}}}. \qquad 11$$

The relative contribution of g_M to the change in C_M is the complement $\rho(g_M)_{C_M} = 1 - \rho(g_S)_{C_M}$. The marginal contribution of C_M to the change in assimilation $\xi(C_M)_A$, calculated by Eqn 3, is split into the g_S component as $\xi(g_S)_A = \xi(C_M)_A\, \rho(g_S)_{C_M}$, and the g_M component, which is the complement $\xi(g_M)_A = \xi(C_M)_A\, \rho(g_M)_{C_M}$. The calculations can be found in Sheet 4 of the workbook. Analogously, this procedure can also be used to analyse the contributions between two ordinary operational condition to compare two ordinary operational conditions (transition 4 in Figure 1b), with finite g_S and g_M, simply change the parameterisation of C_M, g_{S2} and g_{M2} in Sheet 4.

If some plants are subject to a generic treatment it is possible to evaluate stomatal limitation of treated plants by lifting it in a single transition (number 5 in Figure 1b), as shown above. The difference between the potential attained by the treated plant and the healthy plant is referred to as non-stomatal limitation, which is lifted in a second transition (number 6 in Figure 1b). When it is impractical or impossible to A/C_i responses of the treated plant, the operational parameters need to be estimated. In the method that I recently proposed (Bellasio 2023), the A/C_i curve of the treated plant is estimated under the assumptions that the curvature ω and the CO_2 compensation point Γ are not affected by the treatment, while the horizontal asymptote A_{SAT} and the initial slope CE maintain their ratio constant. The unknown A/C_i curve of the treated plant is estimated by 'flattening' the A/C_i curve of the healthy plant to match the pair ($C_{i\,op}$, A_{op}) measured for the treated plant (red line in Figure 2C). If the ratio $\mu = A_{SAT}/CE$ is invariant, then Eqn 1 can be solved for CE as:

$$CE' = \frac{A(\mu + C_\mathrm{i} - \Gamma) + \sqrt{[A(\Gamma - C_\mathrm{i} - \mu)]^2 - \left[4\,\omega\,A^2\,\mu\,(C_\mathrm{i} - \Gamma)\right]}}{2\mu\,(C_\mathrm{i} - \Gamma)}, \qquad 12$$

CE', the estimated value of CE of the treated plant, is directly calculated by inputting measured A_op and C_iop in Eqn 12; A_SAT', the estimated value of A_SAT in the treated plant, is, by assumption, $\mu\ CE'$. The calculations and control analyses are shown for each step in Sheet 5 of the workbook. Alternatively, limitations can be lifted in a single transition between the operational conditions of the treated plant and the potential conditions of the healthy (number 7 in Figure 1b). Calculations are shown in Sheet 10 of the workbook.

If A/C_i curves and g_M are available for both the healthy and the treated plants, diffusional limitation can be resolved in its mesophyll and stomatal components by lifting them in a single transition (number 8 in Figure 1b), while the remaining portion is evaluated as shown previously (number 6 in Figure 1b). A numerical example is shown in Figure 3D, and the corresponding calculations and control analysis are in Sheet 6 of the workbook.

Light and non-light restrictions

Light limitation analysis can be utilized to quantify the reduction of assimilation due to shading, relative to a hypothetical case where the leaf would be exposed to maximum lighting. Similar to the procedure used for stomatal limitation analysis, light response curves are measured under specific growth conditions (CO_2 concentration, temperature, *etc.*). Then, the dependence of assimilation on light intensity is modelled in analogy with Eqn 9 using the empirical model of Prioul and Chartier (1977) in its original formulation, *i.e.* Eqn 2 in Bellasio et al. (2016b), coded in the 'GAvPPFD' Sheet of the provided workbook. Light limitation is quantified by evaluating a single transition between operational conditions, and where light limitation is assumed to be absent (number 1 in Figure 1c). A worked example is provided in Sheet 2. The same procedure is apt for analysing light contributions between two real conditions of interest by specifying the second condition in the parameterization of State II in Sheet 2 (number 2 in Figure 1c). The analysis of light and non-light limitations can be used to distinguish the effect on assimilation directly due to shading from that due to the downregulation of the biochemical potential that occurred in a treated plant. Analogous to the approach used to resolve diffusional and non-diffusional limitations, two variants are possible. In the first case, light limitation is lifted first (number 3 in Figure 1c), and the remainder is the difference with the potential of the healthy plant (number 4 in Figure 1c). Alternatively, limitations are lifted in a single transition (number 5 in Figure 1c, calculated in Sheet 7).

Alternatives

I will now review some of the procedures that have been used in the past to help the reader relate to the current framework, alongside a new alternative.

Stomatal and non-stomatal limitations through invariant C_i

The method of Björkman et al. (1980) can be formalised within this generalised framework. The A/C_i curve for the treated plant is approximated with that of the healthy plant for $C_i > C_{i\,op}$ translated vertically to match the operational assimilation of the measured plant as:

$$f(C, \boldsymbol{b}') \approx f(C, \boldsymbol{b}'') - \left[f\left(C_{iop}, \boldsymbol{b}''\right) - f\left(C_{iop}, \boldsymbol{b}'\right)\right], \qquad 13$$

where $\boldsymbol{b}'$ and $\boldsymbol{b}''$ are the set of parameters of the measured, and reference plant, respectively; $f(C, \boldsymbol{b}')$ is the A/C function to be estimated; $f(C, \boldsymbol{b}'')$ is the known A/C function with the parameters $\boldsymbol{b}''$ determined for the reference plants; the expression in square brackets is the down-translation (Figure 4A). Stomatal and non-stomatal limitation are quantified in two transitions as shown above (Figure 4A). Calculation of Eqn 13 infor each step of the first transition is shown in Sheet 8.

Stomatal and non-stomatal contributions through invariant g_S

Contribution analysis has traditionally been conducted by lifting restrictions independently in two transitions. These may follow two paths, which I have implemented within this framework, further demonstrating its generality and flexibility. The first path assumes that, starting from the operational conditions of the healthy leaf, stomata respond before any change in leaf biochemical processes occurs. Figure 4B illustrates this case, with data from Table 2 (state III is the healthy plant, II has reduced g_S, state I is treated). The second variant assumes that biochemical regulation occurs before stomata respond. In this scenario, there would be an alternative path through state II′ (Figure 4B) where g_S equals that of the healthy plant, while the photosynthetic characteristics are that of the treated plant.

To calculate these transitions, it is required to identify the (C_i, A) coordinates of State II. State II is located at the intersection between the supply and demand functions, which will be equated. First, the leaf supply function is:

$$C_\mathrm{i} = C_\mathrm{a} - \frac{A}{g_\mathrm{s}}. \qquad 14$$

Using Eqn 9 as the demand function, and by combining it with Eqn 12, results in a quadratic for A:

$$A = \frac{CE\left(\frac{A_\mathrm{SAT}{}^2}{g_\mathrm{s}} + C_\mathrm{a} - \Gamma\right) - \sqrt{\left[CE\left(\Gamma - C_\mathrm{a} - \frac{A_\mathrm{SAT}{}^2}{g_\mathrm{s}}\right)\right]^2 - 4\left(\omega + \frac{CE}{g_\mathrm{s}}\right) A_\mathrm{SAT}\, CE\,(C_\mathrm{a} - \Gamma)}}{2\left(\omega + \frac{CE}{g_\mathrm{s}}\right)}. \qquad 15$$

Assimilation at the interception is solved using in Eqn 15 the g_S relevant to each of the two cases; the corresponding C_i is found by solving Eqn 14. These cases are calculated in Sheet 9 and 10 in the order I→II→III, in reverse order they simply change sign.

Mechanistic models

Mechanistic models are typically more complicated than empirical, rely on a number of assumptions, are valid only when assumptions hold (*e.g.* a C_4 model is not meaningful for mechanistically describing C_3 plants) and they are less flexible in data fitting. However, they are needed to resolve which processes other than diffusion are causing photosynthetic restrictions. Well-thought procedures are needed, which should be designed specifically to target the experimental question, and cannot be fully described here. However, to show the rationale and facilitate this task, I will exemplify the basic mechanistic models of C_3 assimilation and of C_4 assimilation. These allow to relatively simple partitioning of non-diffusional restriction, such as distinguishing between restrictions due to light reactions or carbon metabolism.

Mesophyll, stomatal, and non-diffusional contributions with a C_3 mechanistic model

This method is essentially the method presented by Buckley and Diaz-Espejo (2015), framed within this generalised set of definitions, and differs from the analysis of mesophyll, stomatal, and non-diffusional contributions exemplified above only in that it uses the C_3 mechanistic model developed by Farquhar et al. (1980). This model has previously been used for the analysis of limitations imposed by Rubisco activation in its enzyme limited submodel (Deans et al. 2019) or in the full formulation (Taylor and Long 2017), and can also be used to quantify limitations imposed by electron transport (Buckley and Diaz-Espejo 2015). However, this method is less widely applicable than the empirical procedure described above: it is meaningful only for C_3 plants; obtaining specific values for the Rubisco Michaelis-Menten constants for carboxylation and oxygenation (K_C and K_O) for measured leaves may not be readily achievable, and the cut-off point for enzyme and light limitation must be assumed. Therefore, it is recommended only for cases where a mechanistic description of C_3 assimilation is specifically required. Calculations and a brief explanation of how parameters were derived for the gas exchange example in Table 2 are included in Sheet 12.

C_4 mechanistic model

A C_4 mechanistic model may serve for the quantification of restrictions due to diffusion through stomata or the mesophyll, as well as restrictions caused by other factors like light intensity, the light-saturated rate of ATP generation (J_{SAT}), the curvature of the light dependence of ATP generation (θ), the initial quantum yield for ATP generation $Y(J_{ATP})_{LL}$, respiration in the light, Rubisco and phosphoenolpyruvate carboxylase CO_2 saturated rate of carboxylation (V_{CMAX} and V_{PMAX}), the factor that partitions ATP between PEP regeneration and the remainder of photosynthetic activity (x), and bundle sheath conductance (g_{BS}). For example, it can be used to determine the contribution of light versus that of g_{BS} in the reduction of assimilation for plants grown under shading (Bellasio and Griffiths 2014b). The formulation of Berry and Farquhar (1978)

in the corrected version of Bellasio et al. (2017) is coded in Sheet 13, and its implementation is the same as in previous analyses.

More complex scenarios

For conducting more in-depth analyses of non-diffusional restrictions and evaluating a broad range of sophisticated questions I recommend utilizing the Bellasio and Farquhar (2019) and Bellasio and Ermakova (2022) analytical models. The analytical model of Bellasio and Farquhar (2019) allows the quantification of limitations imposed by a wide range of real or imagined scenarios, in any photosynthetic type (C_3, C_2, C_2+C_4, C_4), intermediates thereof, and engineered transitions between them, stomatal opening and closure, different stomatal responsiveness to biochemical forcing or drought, and a wide range of characteristics of the electron transport chain (*e.g.* shifting the ratio between ATP and NADPH production by modifying the fraction of cyclic electron flow or the NDH pathway, *etc*.). The analytical model of C_4 photosynthesis of Bellasio and Ermakova (2022) relates to leaf anatomy following Bellasio and Lundgren (2016) and explicitly accounts for light harvesting partitioning between cell compartments. It was specifically developed for studying differences between C_4 photosynthetic subtypes, and maintains validity at very low irradiance. It features two electron transport chains, C_4 cycle reactions, and C_3 cycle reactions accommodating a variety of possibilities for parameterisation. These models are coded in intuitive spreadsheets available for free download from the publisher's website, and they can be seamlessly incorporated into the workbook provided here.

Discussion

I set out to generalise the analyses of photosynthetic restrictions, providing a set of definitions that integrate several common and new procedures. Ideally, a quantitative assessment of the accuracy of this new framework's performance would be desirable; however, this is impossible because there is no absolute reference for comparison. Therefore, I minimized practical details and used synthetic data instead of experimental data to illustrate applications. These examples should not be passed as proof of validity, although that is common practice in the literature. To avoid confusion, I will evaluate the new framework solely from a logical standpoint.

I start by stating the objective desirability criteria for restriction analyses: they should be general, theoretically sound, and univocal. The new framework is general, as it is valid for all photosynthetic types and models, and it comprehensively quantifies limitations, contributions, and controls (sensitivity and elasticity) within a single procedure. The framework avoids two erroneous practices: that of approximating curves with lines in finite intervals, and that of misestimating their slopes. This practice was introduced by Tomás et al. (2013) and gained traction in later studies, for instance by Tosens et al. (2016), Carriquí et al. (2015). The slope of the A/C_i response curves required for the linear approximation of Grassi and Magnani (2005) was measured under low CO_2

concentrations – where it is typically several-fold higher than under ordinary operational conditions. This inevitably leads to largely overestimating the importance of diffusion, whether across stomata or through the mesophyll, and has likely brought to overstating their importance in controlling assimilation. The third criterion of univocity is the most delicate, requiring detailed discussion. Many of the applications I presented, such as diffusional limitation and light limitation analyses, are evaluated by formulating calculations so that only one quantity (variable a in Eqn 1) varies between transitions, while the parameterization remains constant (vector $\boldsymbol{b}$ in Eqn 1). In all those cases the method is unequivocal, and equivalent both for limitation and contribution analysis. When multiple quantities vary, methodological variants are possible (the number of variables changing raised to the power of the number of transitions), but it is still generally possible to define how to proceed.

In contribution analysis, it had been proposed to assume that stomata respond before any change in leaf biochemical processes occurs, or the reverse. The difference in assimilation between states where only g_S changed (in Figure 4B, A_I-A_{II} in the path 'stomata first' or $A_{II'}$-A_{III} in 'mesophyll first') equals to the contribution of C_i to the change in assimilation, $\Xi(C_i)_A$ (-0.9 μmol m^{-2} s^{-1} in 'stomata first' or -0.6 μmol m^{-2} s^{-1} in 'mesophyll first') because only g_S varied in the corresponding transition. Conventionally, this has been taken as the overall stomatal contribution compounding both transitions, because $\Xi(C_i)_A$ has been assumed zero for transitions at constant g_S. This mistake that has been systematically made – and since overlooked – for both the 'stomata first' and 'mesophyll first' paths (Prioul et al. 1984). In the transitions at constant g_S, $\Xi(C_i)_A$ was even higher in magnitude than in the transitions at variable g_S (1.8 μmol m^{-2} s^{-1} in 'stomata first' or 1.6 μmol m^{-2} s^{-1} in 'mesophyll first'). As a result, the compounded $\Xi(C_i)_A$ over the two transitions was positive for both paths, meaning the treated was less stomatally limited than the healthy state, despite the lower g_S (as in the path-independent evaluation, Figure 3D).

The discrepancy between paths, in contrast to previous reports *e.g.* five-fold in Assmann (1988), was relatively small, about 20% (0.83 μmol m^{-2} s^{-1} in 'stomata first' or 1.1 μmol m^{-2} s^{-1} in 'mesophyll first'). Therefore, the choice between paths is not critical. Yet, even if correctly implemented, path dependent variants are not recommended. While their assumptions may partially hold under specific conditions, such as when stomatal adjustment is much slower than photosynthetic activation (Deans et al. 2019), they are generally invalid. During the imposition of a treatment, photosynthetic characteristics typically respond progressively, driven by a common factor – the treatment – and are therefore not independent. They can be presumed to change concurrently and linearly between their initial and final values (number 3 in Figure 1b), as proposed by Buckley and Diaz-Espejo (2015), thus eliminating ambiguity in contribution analysis.

In the analysis of limitations, flexibility is necessary. Much of the past debate has been driven by methodological papers, which naturally prioritize showcasing the breadth of alternative approaches rather than narrowing their choice. I suggest shifting the focus to the experiment itself and its questions; in most cases, the appropriate method will naturally and unambiguously emerge from

them. Whenever the effects of the treatment are stable, restrictions should be lifted first. This principle broadly applies to situations where plants are subject to permanent or mid-term acclimation treatments (*e.g.*, differing nitrogen levels, watering levels, growth light conditions, growth CO_2 levels, soil types, fertilisation, mycorrhization, *etc.*), or differ by any genetic trait, whether natural or engineered. These traits are not subject to short-term changes, and it is possible to devise a hypothetical scenario whereby limitations are lifted independently, assuming the characteristics of the plant remain constant. Applying this principle involves evaluating two transitions (numbers 5 and 6 in Figure 1b), which is the conventional approach used in the literature.

I presented a novel single-transition variant for limitation analysis (number 7 in Figure 1b), which has the benefit of being unequivocal and could therefore resolve any doubt about the order in which limitations are lifted. Compared to the path-dependent method (Sheet 5), the relative stomatal contribution $\rho(g_S)_A$ was slightly higher with the single transition (0.5 vs. 0.44), but the magnitude of the difference was relatively small, about 10%. This means that this method can be safely used whenever there is doubt about the path to follow in limitation removal. However, despite these benefits, I cannot think of a specific case where this variant should be chosen over the two-tiered transition, which I think is preferable.

Limitation analysis requires the parameterization vector $\boldsymbol{b}$ to be known for the treated plants. For instance, in the case of stomatal and non-stomatal limitation analysis, this involves measuring the A/C_i responses of both the healthy and the treated plant. Through an elegant experimental routine, Taylor and Long (2017) measured rapid A/C_i responses in real time during the treatment's course, using modern gas exchange equipment and routines (Stinziano et al. 2017). However, often it is impractical or impossible to measure A/C_i responses of treated plants; in which case the parameterization must be estimated. A simple and widely used method is that of Björkman et al. (1980), which assumes that lifting stomatal limitation in the treated plant would result in the same increase in assimilation as in the healthy plant (this corresponds to estimating the A/C_i curve of the treated plant by 'copying' that of the healthy plant for $C_i > C_{iop}$, Eqn 13). This simplification is generally acceptable for C_4 plants because A/C_i curves are flat for $C_i > C_{iop}$. For C_3 plants, it may be acceptable only when the treatment effect is small, but it overestimates stomatal limitation when their assimilatory potential is substantially reduced. The recommended alternative, based on Bellasio (2023) involves flattening the A/C_i curves of treated plants (Eqn 12). The simplification I proposed to scale CE and A_{SAT} is based on the necessity of an analytical solution, and on the observation that Γ and ω did not significantly change in both C_3 and C_4 plants during seasonal drought (Bellasio et al. 2022). It may not have general validity, as the treatment's effect on parameters may be species- and treatment-dependent. However, the improvement attainable by using actual values may not be substantial.

The analysis of light and non-light restrictions is original to this study. Lifting light limitation may not involve exposing leaves to infinite light intensity but just to full sunlight, making it difficult to pinpoint the real versus hypothetical conditions, creating confusion between contribution and limitation analyses. A decrease in assimilation may result from a combination of direct and indirect effects of shading, such has the decrease in biochemical potential that occurs in a leaf shaded by the overgrowth of a new canopy (Bellasio and Griffiths 2014a). Because these responses are not independent, in this case the analysis of contributions in a single transition may be appropriate. Alternatively, if the treatment has affected the biochemical potential independently of light, such as in cases of pathogen attack or nitrogen level changes (Dewar et al. 2012), then limitation analysis with a two-tiered transition may be preferable.

Conclusion

I urge the community to critically reevaluate the relative importance of stomatal, mesophyll, and non-diffusional restrictions, especially when they were evaluated using the linear approximation in finite intervals by Grassi and Magnani (2005), and the initial slopes of the A/C_i curves by Tomás et al. (2013), which are erroneous. I recommend using the theoretical framework of Eqn 1-8 either in single transitions (when only one input changes and for contribution analysis) or by lifting limitations first (for limitation analysis). Common procedures are coded in Sheets 1 to 7 of the provided workbook.

Availability

The spreadsheet with calculation is available in the Supporting Information of this article. A curated version is available on GitHub at the link [add link]. A video tutorial is available on YouTube at the link [add link].

Acknowledgments

This work slowly emerged from the requests I received during the four years of the troubled gestation of my previous commentary, eventually expanding into a standalone paper. Reaching this point would have been impossible without the trust of Editor Patrick Morgan and the patience of the reviewers, who managed to navigate my early drafts at various stages. I am grateful to Hilary Stuart-Williams, Ross Deans, and Jaume Flexas for their valuable discussions.

I have no competing interests.

Funding

I gratefully acknowledge funding by a Science Foundation Ireland Individual Pathway Fellowship (21/PATH-S/9322), and by a European Union's Horizon 2020 research and innovation programme MSCA individual fellowship (grant agreement ID No: 702755).

461 **Table 1. Acronyms, definitions, variables, and units used.**

Symbol	Definition	Units
a	any generic input of a mathematical model	
A, A_{op}	Net assimilation, unspecified or measured under ordinary, operational conditions	µmol CO_2 m^{-2} s^{-1}
A_{SAT}, A_{SAT}'	CO_2 saturated A, unspecified of after a generic treatment, respectively	µmol $CO_2 m^{-2}$ s^{-1}
$\boldsymbol{b}$	a generic set of inputs of a mathematical model which includes all parameters and variables that are not a	
C_a	CO_2 concentration outside the leaf	µmol CO_2 mol air^{-1}
CE, CE'	Initial slope of the A/C_i curve, unspecified of after a generic treatment, respectively	mol air m^{-2} s^{-1}
C_i, C_{iop}	CO_2 concentration in the substomatal cavity as calculated by the IRGA, unspecified, or under operational conditions	µmol CO_2 mol air $^{-1}$
C_M	CO_2 concentration at the mesophyll carboxylating sites	µmol CO_2 mol air $^{-1}$
Contribution	Any change in an output variable which is due to a change only in one input, it can be marginal [small csi, ξ, Eqn 3], total [capital csi, Ξ, Eqn 4], or relative [eta, η, Eqn 5].	µmol m^{-2} s^{-1}, the relative is dimensionless
E	Leaf level water transpiration rate	mmol H_2O m^{-2} s^{-1}
g_{BS}	Bundle sheath conductance to CO_2 diffusion	mol m^{-2} s^{-1}
g_M	Mesophyll conductance to CO_2 diffusion	mol air m^{-2} s^{-1}
g_S	Stomatal conductance, here to CO_2 diffusion also when unspecified, elsewhere often referred to as g_{SC}	mol air m^{-2} s^{-1}
g_{Tot}	Total conductance to CO_2 diffusion, the reciprocal of g_{Tot} is the sum of the reciprocal of g_S plus the reciprocal of g_M	µmol m^{-2} s^{-1}
k, K	Any generic interval between states and the total number of intervals, respectively	
Limitation	The total contribution divided by the maximum value of the function in the interval, Eqn 6	
L_{NS}	Non-stomatal limitation to photosynthesis	dimensionless
L_S	Stomatal limitation to photosynthesis	dimensionless
m, M	Any generic state, and the total number of states, respectively	
Restriction	Any generic hindrance to photosynthetic activity	
Sensitivity	The marginal contribution divided by the value of the variable, relative to the change in input divided by the value of the input, Eqn 7	
State	Any condition in which a photosynthetic model can be defined (by knowing a and $\boldsymbol{b}$)	
μ	A_{SAT} divided by CE	
Ω	Any generic output of a mathematical model, a function of a and $\boldsymbol{b}$	
ω	Curvature of the non-rectangular hyperbola describing the C_i dependence of A	dimensionless

462

Table 2. Synthetic data used in the examples. Plants were either untreated or subjected to a hypothetical treatment which reduced the photosynthetic potential. The rates of assimilation (A) and CO_2 concentration in the substomatal cavity (C_i) attained in the conditions in which plants were grown are denoted as operational. Gas exchange measurements at the lab bench determined the responses of A to C_i. Values of CO_2 concentration at the sites of carboxylation was calculated using mesophyll conductance values of 0.35 mol m^{-2} s^{-1} and 0.25 mol m^{-2} s^{-1}, previously obtained for healthy plants and treated plants, respectively. Assimilation is expressed in µmol m^{-2} s^{-1}, CO_2 concentration in µmol mol^{-1}. Non-rectangular hyperbolas were fitted either to the A/C_i or to A/C_M curves to obtain two sets of fitted parameters reported at the bottom using the fitting tool of Bellasio et al. (2016b), copied in the sheet 'AvCi' of the workbook provided in Supporting Information for convenience.

Measured	**Healthy**			**Treated**		
Operational	A_{op}	$C_{i\ op}$	$C_{M\ op}$	A_{op}	$C_{i\ op}$	$C_{M\ op}$
	13.9	200	160	11	220	176
A/C Response	A	C_i	C_M	A	C_i	C_M
	-2.59	24	32	-1.91	24	32
	-1.22	35	38	-0.90	35	39
	0.60	50	48	0.44	50	48
	3.00	71	62	2.21	71	62
	6.15	101	84	4.53	101	83
	10.1	145	116	7.42	145	115
	14.4	210	166	10.6	210	164
	17.9	294	243	13.2	294	242
	20.7	420	361	15.2	420	359
Fitted		**C_i-based**	**C_M-based**		**C_i-based**	**C_M-based**
A_{SAT} / µmol m^{-2} s^{-1}		26	26		19	19
CE / mol m^{-2} s^{-1}		0.12	0.18		0.09	0.14
ω		0.7	0.54		0.7	0.54
Γ / µmol mol^{-1}		45	45		45	45

Figure 1. Generalised framework of restriction analysis.

Restrictions may be evaluated along a real and an hypothetical dimensions. The analysis of limitations quantifies the restriction independently in each plant, compared their maximum potential. The analysis of contribution analyses the transition between two real conditions. The analysis of control (sensitivity and elasticity) can be done at any intermediate points of the transitions (exemplified by a 'C' in a green circle that may be swinging over all arrows). Panel (a) general framework; Panel (b) diffusional and non-diffusional restrictions; Panel (c) light and non-light restrictions.

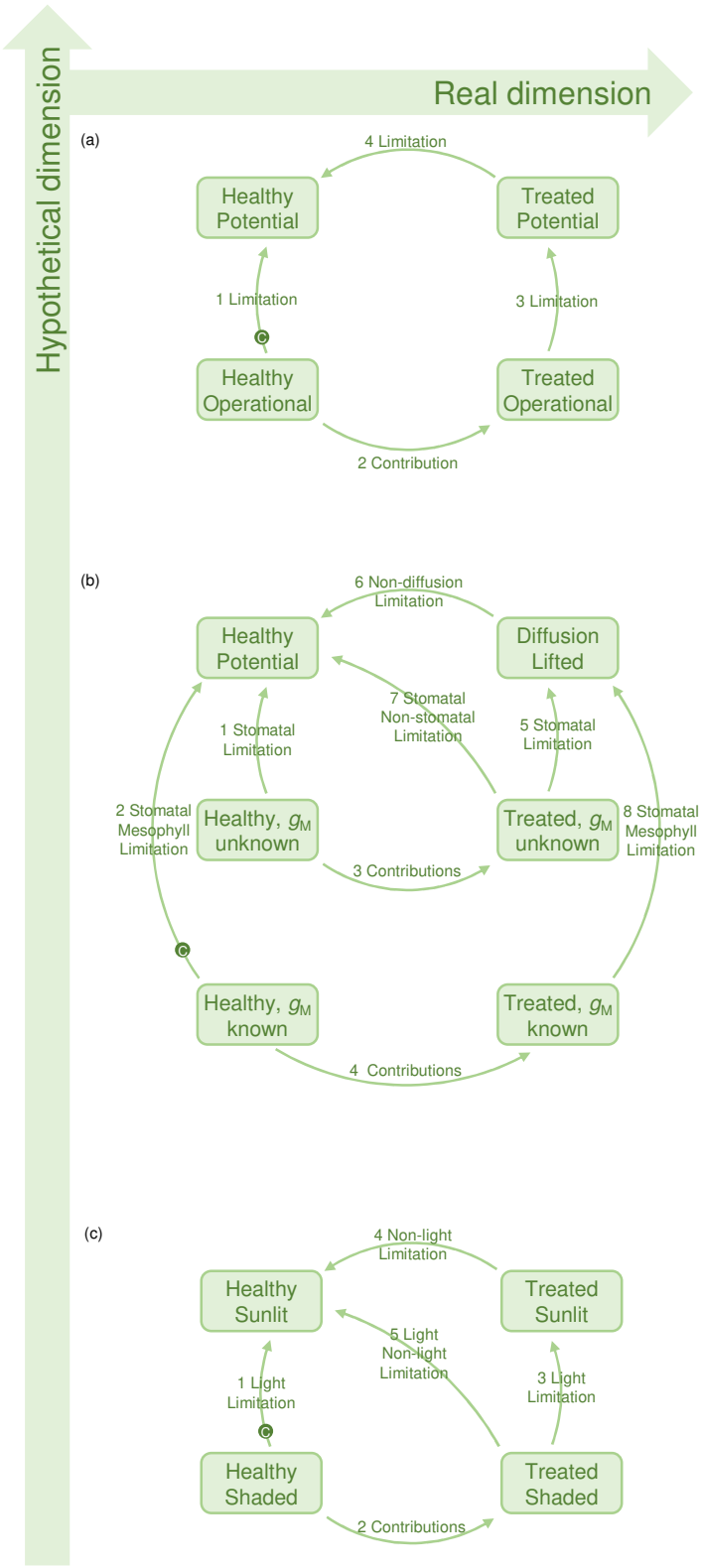

Figure 2. Schematic of the generalised framework of definitions.

A generic output variable Ω is described through a mathematical model as a function of the variable a (in abscissa) and a set of other inputs $\boldsymbol{b}$. The conditions in which a and **b** are known are called 'states', here represented by two black diamonds. The function $\Omega = f(a, \boldsymbol{b})$ parameterised with the known vector $\boldsymbol{b}$, for state I is shown in red, and for state II is shown in blue. The transition between the two known states is divided in four equal intervals, which are bordered by thin black lines. The value of the inputs a and $\boldsymbol{b}$ is assumed to vary linearly in the intervals. The marginal contribution ξ of the variable a to the change in the output Ω is shown in purple. The value of ξ' becomes equal to that of ξ for large values of K.

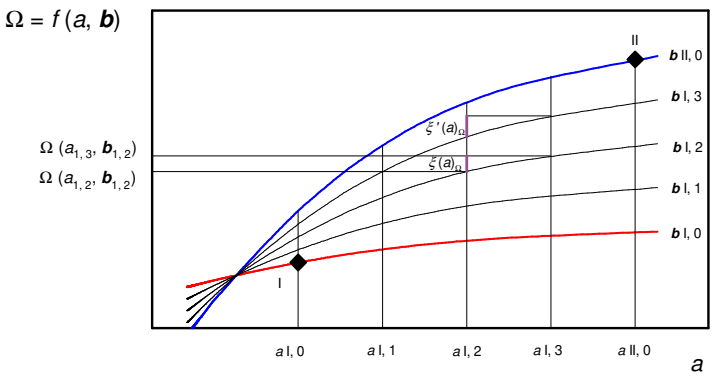

Figure 3. Quantifying limitations and contributions to changes in photosynthesis

Stomatal limitation. Panel **A** shows a photosynthetic model describing the dependence of assimilation (A) upon CO_2 concentration in the substomatal cavity (C_i, solid line, Eqn 9) of healthy plants (blue). In this example with hypothetical data, operational conditions correspond to an ambient CO_2 concentration (C_a) of 420 µmol mol^{-1} and a fixed light intensity (the level is irrelevant here). It attains a rate of assimilation (A_{op}) of 13.9 µmol m^{-2} s^{-1}, and has a CO_2 concentration in the substomatal cavity ($C_{i\ op}$) of 200 µmol mol^{-1}, corresponding to an operational stomatal conductance to CO_2 $\left[g_{SC\ op} = \frac{A_{op}}{C_a - C_{i\ op}}\right]$ of 0.063 mol m^{-2} s^{-1} (Table 2). In the transition between operational State I and hypothetical State II assimilation is driven to its potential as if intercellular spaces were directly exposed to external CO_2 concentration, C_a (Eqn 9 calculated for $C_i = C_a$). Assimilation increased from 13.9 to 20.7 µmol m^{-2} s^{-1}; the total contribution of C_i to the change in assimilation $[\Xi(C_i)_A]$ was 6.9 µmol m^{-2} s^{-1}; the relative contribution of C_i to the change in assimilation $[\rho(C_i)_A]$ was 1 because C_i was the only input to vary between the two states; the limitation imposed by C_i to assimilation $[L(C_i)_A]$ corresponds to stomatal limitation, was 0.33. $S(\Omega)_a$, and $\eta(\Omega)_a$ are shown in Sheet 1, calculated for each step of the transition.

Diffusional limitation. Panel **B** shows the modelled dependence of assimilation (A) upon CO_2 concentration in the mesophyll (C_M, dashed line, Eqn 9) of healthy plants. Diffusional limitation is quantified by evaluating transitions from the operational conditions of state I where C_M corresponds to $C_{M\ op}$, to a state II where the hindrance to CO_2 diffusion caused both by the stomata and by the mesophyll is removed. Assimilation increased from 13.9 in state I, to 21.5 µmol m^{-2} s^{-1} in state II; diffusional limitation was 0.36; details are in Sheet 3 of the workbook. Diffusional limitation is then partitioned into its mesophyll and stomatal components in Sheet 4.

Stomatal and non-stomatal limitation. Panel **C** shows the modelled A/C_i curves of healthy (blue) and treated (red) plants. State I is the operational conditions of the treated plant (diamond 'I'). State II is where, with otherwise invariant parameterisation, the stomatal barrier is removed by driving C_i to the value of C_a of 420 µmol mol^{-1}. State III is where C_a is invariant, while the parameters A_{SAT} and CE are driven to those of the reference plant. The treated plant had an A_{op} of 11 µmol m^{-2} s^{-1}, and a $C_{i\ op}$ of 220 µmol mol^{-1}, the healthy plant is the same (Table 2). In the transitions, assimilation increased from A_{op} of 11 in state I, to A_{Ca} of 15.2 µmol m^{-2} s^{-1}in state II to A_{Pot} of 20.7 µmol m^{-2} s^{-1} in state III. The limitation of C_i to assimilation $L(C_i)_A$, that is, stomatal limitation, was 0.20; the sum of the other limitations (A_{SAT}, CE, ω, and Γ), that is, non-stomatal limitation, was 0.26. Calculations are shown in Sheet 10 of the workbook. In the corresponding single transition stomatal limitation was 0.23, non-stomatal limitation was 0.23 (Sheet 11).

Contribution analysis. Panel **D** shows the modelled A/C_M curves of healthy (blue) and treated plants (red). Healthy plants' A/C_M responses, A_{op}, $C_{M\ op}$, $g_{SC\ op}$ and g_M are from previous examples while $g_{SC\ op}'$ was 0.055 mol m^{-2} s^{-1}. Parameters of the fitted to A/C_M responses are in Table 2. State I and II represent generic operational points of healthy and treated plants, respectively. Stomatal, mesophyll and non-diffusional contribution are quantified in a single transition whereby quantities change linearly between values of healthy and treated plants. Although the treatment reduced both

g_S and g_M, C_M was higher in the treated plant than in the healthy, therefore, the total diffusional contribution was positive (0.9 µmol m^{-2} s^{-1}), resolved in a stomatal contribution of 0.5 µmol m^{-2} s^{-1}, and a mesophyll contribution of 0.4 µmol m^{-2} s^{-1}. The total non-diffusional contribution was -3.73 µmol m^{-2} s^{-1}. The calculations are in Sheet 6.

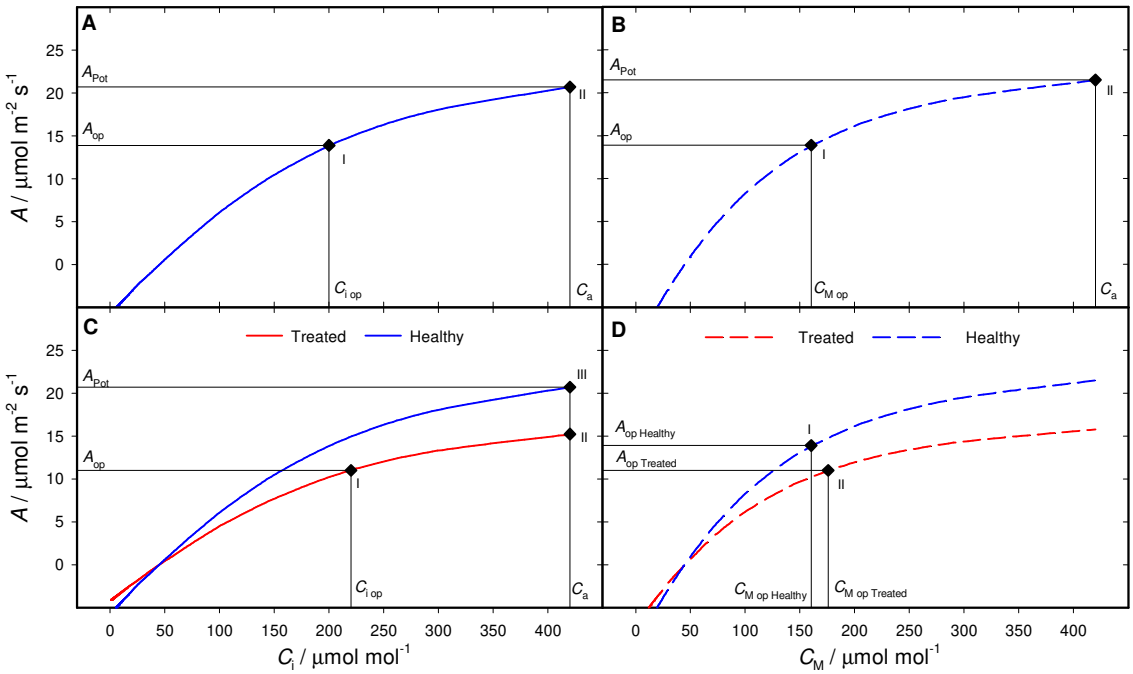

Figure 4. Alternative path dependent methods

Panel **A** shows the method of Björkman et al. (1980). The A/C_i curve for the treated plant (in red) is approximated with that of the healthy plant (in blue) for $C_i > C_{i\,op}$. A_{op} is the rate of assimilation of the treated plant in operational conditions, $f\left(C_{iop}, \boldsymbol{b}'\right)$ in Eqn 13; $A_{Pot\,Ci}$, is the rate of assimilation that the healthy plant would have if C_i were that of the treated plant in the operational condition C_{iop},, $f\left(C_{iop}, \boldsymbol{b}''\right)$ in Eqn 13; A_{Pot} is that a healthy plant would have in absence of stomatal barrier, $f(C_a, \boldsymbol{b}'')$ in Eqn 13. Limitations are evaluated by removing stomatal limitation first in the transition between state I and state II, and then by removing non-stomatal limitation in the transition between state II and state III. The conventional three point calculation (Bellasio et al. 2023) gives the same results as the current framework: the total stomatal contribution $\Xi(C_i)_A$ is $A_{Pot} - A_{Pot\,Ci}$, and the total non-stomatal contribution $\Xi(L_{NS})_A$ is $A_{Pot\,Ci} - A_{op}$ (Sheet 8).

Panel **B** shows two path-dependent variants of contribution analysis where a healthy plant (in blue) undergoes a generic treatment that restrict assimilation (in red). State I and III represents a generic operational point of the treated plant, and healthy plant, respectively, while state II is an intermediate state through which the transition is assumed to occur. The first path assumes that in response to the treatment stomata respond before any change in leaf biochemical processes occurs, that is, a transition from state III to state II, with reduced g_S, and then to state I, with lower photosynthetic potential but equal g_S. The second variant assumes that biochemical regulation occurs before stomata respond, that is, a path through state II′ where g_S equals that of the healthy plant, while the parameterization corresponds to that of the treated plant. In the path 'stomata first' during the transition between state I and state II, $\Xi(C_i)_A$ was -0.9 µmol m^{-2} s^{-1} (L_S increased); during the transition between state II and state III, $\Xi(C_i)_A$ was 1.8 µmol m^{-2} s^{-1} (L_S decreased even if g_S did not change). In the path 'mesophyll first' during the transition between state I and state II′, $\Xi(C_i)_A$ was 1.6 µmol m^{-2} s^{-1} (L_S decreased even if g_S did not change); during the transition between state II and state III, $\Xi(C_i)_A$ was -0.6 µmol m^{-2} s^{-1} (L_S increased). The calculations are in Sheets 9 and 10.

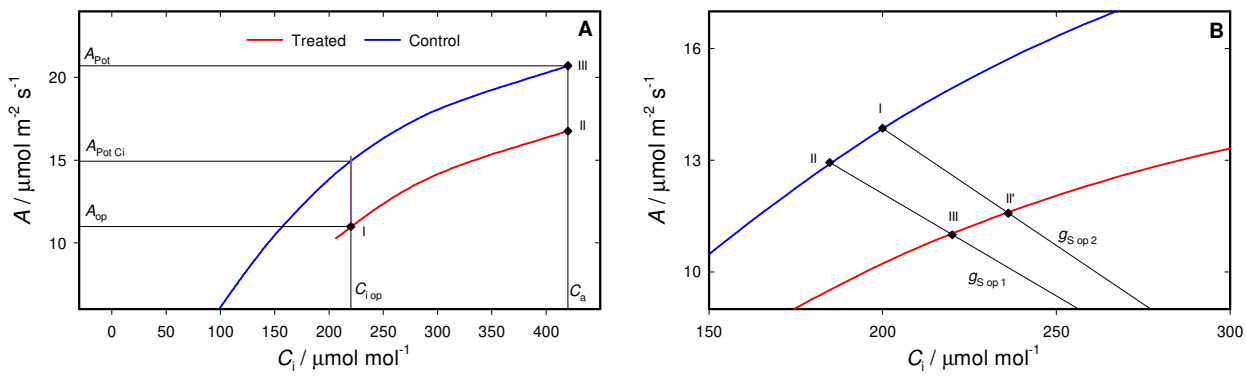

References

Assmann S (1988) Stomatal and non‐stomatal limitations to carbon assimilation: an evaluation of the path‐dependent method. Plant, Cell & Environment 11 (7):577-582.

Bellasio C (2023) The slope of assimilation rate against stomatal conductance should not be used as a measure of water-use efficiency or stomatal control over assimilation. Photosynth Res 158:195-199.

Bellasio C, Beerling DJ, Griffiths H (2016a) Deriving C_4 photosynthetic parameters from combined gas exchange and chlorophyll fluorescence using an Excel tool: theory and practice. Plant, Cell & Environment 39 (6):1164-1179.

Bellasio C, Beerling DJ, Griffiths H (2016b) An Excel tool for deriving key photosynthetic parameters from combined gas exchange and chlorophyll fluorescence: theory and practice. Plant Cell Environ 39 (6):1180–1197.

Bellasio C, Ermakova M (2022) Reduction of bundle sheath size boosts cyclic electron flow in C4 Setaria viridis acclimated to low light. The Plant Journal 111 (5):1223-1237.

Bellasio C, Farquhar GD (2019) A leaf-level biochemical model simulating the introduction of C2 and C4 photosynthesis in C3 rice: gains, losses and metabolite fluxes. New Phytologist 223 (1):150-166.

Bellasio C, Griffiths H (2014a) Acclimation of C4 metabolism to low light in mature maize leaves could limit energetic losses during progressive shading in a crop canopy. Journal of Experimental Botany 65 (13):3725-3736.

Bellasio C, Griffiths H (2014b) Acclimation to Low Light by C4 maize: Implications for Bundle Sheath Leakiness. Plant Cell Environ 37 (5):1046-1058.

Bellasio C, Lundgren MR (2016) Anatomical constraints to C4 evolution: light harvesting capacity in the bundle sheath. New Phytologist 212 (2):485–496.

Bellasio C, Quirk J, Beerling DJ (2018) Stomatal and non-stomatal limitations in savanna trees and C4 grasses grown at low, ambient and high atmospheric CO2. Plant Science 274:181-192.

Bellasio C, Quirk J, Buckley TN, Beerling D (2017) A dynamic hydro-mechanical and biochemical model of stomatal conductance for C4 photosynthesis. Plant Physiol 175 (1):104-119.

Bellasio C, Quirk J, Ubierna N, Beerling DJ (2022) Physiological responses to low CO2 over prolonged drought as primers for forest-grassland transitions. Nature Plants 8:1014–1023.

Bellasio C, Stuart-Williams H, Farquhar GD, Flexas J (2023) C4 maize and sorghum are more sensitive to rapid dehydration than C3 wheat and sunflower. New Phytologist 240 (6):2239-2252.

Berry JA, Farquhar GD (1978) The CO2 concentrating function of C4 photosynthesis: a biochemical model. In: Hall D, Coombs J, Goodwin T (eds) Proceedings of the 4th International Congress on Photosynthesis, Reading, 1978. Biochemical Society, London, pp 119-131

Björkman O, Downton WJS, Mooney HA (1980) Response and adaptation to water stress in Nerium oleander. Carnegie Institute Washington Yearbook 79:150–157.

Buckley TN, Diaz-Espejo A (2015) Partitioning changes in photosynthetic rate into contributions from different variables. Plant, Cell & Environment 38 (6):1200-1211.

Busch FA (2018) Photosynthetic gas exchange in land plants at the leaf level. Photosynthesis: methods and protocols:25-44.

Busch FA, Holloway-Phillips M, Stuart-Williams H, Farquhar GD (2020) Revisiting carbon isotope discrimination in C3 plants shows respiration rules when photosynthesis is low. Nature Plants 6 (3):245-258.

Cano FJ, Sharwood RE, Cousins AB, Ghannoum O (2019) The role of leaf width and conductances to CO2 in determining water use efficiency in C4 grasses. New Phytologist 223 (3):1280-1295.

Carriquí M, Cabrera HM, Conesa MÀ, Coopman RE, Douthe C, Gago J, GallÉ A, GalmÉS J, Ribas-Carbo M, TomÁS M, Flexas J (2015) Diffusional limitations explain the lower photosynthetic capacity of ferns as compared with angiosperms in a common garden study. Plant, Cell & Environment 38 (3):448-460.

Deans RM, Farquhar GD, Busch FA (2019) Estimating stomatal and biochemical limitations during photosynthetic induction. Plant, Cell & Environment 42 (12):3227-3240.

Dewar RC, Tarvainen L, Parker K, Wallin G, McMurtrie RE (2012) Why does leaf nitrogen decline within tree canopies less rapidly than light? An explanation from optimization subject to a lower bound on leaf mass per area. Tree Physiology 32 (5):520-534.

Farquhar GD, Sharkey TD (1982) Stomatal Conductance and Photosynthesis. Annual Review of Plant Physiology and Plant Molecular Biology 33:317-345.

Farquhar GD, von Caemmerer S, Berry JA (1980) A biochemical-model of photosynthetic CO2 assimilation in leaves of C3 species. Planta 149 (1):78-90.
Gaastra P (1959) Photosynthesis of crop plants as influenced by light, carbon dioxide, temperature, and stomatal diffusion resistance. Veenman,
Grassi G, Magnani F (2005) Stomatal, mesophyll conductance and biochemical limitations to photosynthesis as affected by drought and leaf ontogeny in ash and oak trees. Plant, Cell & Environment 28 (7):834-849.
Gu L, Sun Y (2014) Artefactual responses of mesophyll conductance to CO2 and irradiance estimated with the variable J and online isotope discrimination methods. Plant, Cell & Environment 37 (5):1231-1249.
Jarvis P (1971) The estimation of resistances to carbon dioxide transfer. Plant photosynthetic production Manual of methods.
Jones H (1985) Partitioning stomatal and non‐stomatal limitations to photosynthesis. Plant, Cell & Environment 8 (2):95-104.
Jones H, Slatyer R (1972) Estimation of the transport and carboxylation components of the intracellular limitation to leaf photosynthesis. Plant Physiol 50 (2):283-288.
Jones HG (1973) Limiting factors in photosynthesis. New Phytologist 72 (5):1089-1094.
Márquez DA, Stuart-Williams H, Farquhar GD (2021) An improved theory for calculating leaf gas exchange more precisely accounting for small fluxes. Nature Plants 7 (3):317-326.
Prioul J, Cornic G, Jones H Discussion of stomatal and non stomatal components in leaf photosynthesis decline under stress conditions. In: Advances in Photosynthesis Research: Proceedings of the VIth International Congress on Photosynthesis, Brussels, Belgium, August 1–6, 1983. Volume 4, 1984. Springer, pp 375-378
Prioul JL, Chartier P (1977) Partitioning of Transfer and Carboxylation Components of Intracellular Resistance to Photosynthetic CO2 Fixation: A Critical Analysis of the Methods Used. Ann Bot-London 41 (4):789-800.
Stinziano JR, Morgan PB, Lynch DJ, Saathoff AJ, McDermitt DK, Hanson DT (2017) The rapid A–Ci response: photosynthesis in the phenomic era. Wiley Online Library,
Taylor SH, Long SP (2017) Slow induction of photosynthesis on shade to sun transitions in wheat may cost at least 21% of productivity. Philosophical Transactions of the Royal Society B: Biological Sciences 372 (1730):20160543.
Tomás M, Flexas J, Copolovici L, Galmés J, Hallik L, Medrano H, Ribas-Carbó M, Tosens T, Vislap V, Niinemets Ü (2013) Importance of leaf anatomy in determining mesophyll diffusion conductance to CO2 across species: quantitative limitations and scaling up by models. Journal of experimental botany 64 (8):2269-2281.
Tosens T, Nishida K, Gago J, Coopman RE, Cabrera HM, Carriquí M, Laanisto L, Morales L, Nadal M, Rojas R, Talts E, Tomas M, Hanba Y, Niinemets Ü, Flexas J (2016) The photosynthetic capacity in 35 ferns and fern allies: mesophyll CO2 diffusion as a key trait. New Phytologist 209 (4):1576-1590.
Ubierna N, Gandin A, Boyd RA, Cousins AB (2017) Temperature response of mesophyll conductance in three C4 species calculated with two methods: 18O discrimination and in vitro Vpmax. New Phytologist 214 (1):66–80.
von Caemmerer S, Farquhar GD (1981) Some Relationships between the Biochemistry of Photosynthesis and the Gas-Exchange of Leaves. Planta 153 (4):376-387.